Proceedings of the 7th International Symposium on Cavitation
CAV2009 – Paper No. 152
August 17-22, 2009, Ann Arbor, Michigan, USA

Experimental Study on the Effects of Viscosity and Viscoelasticity on a Line Vortex Cavitation

Charlotte Barbier
DYNAFLOW INC.
Jessup, MD, USA
charlotte@dynaflow-inc.com

Georges Chahine
DYNAFLOW INC.
Jessup, MD, USA
glchahine@dynaflow-inc.com

ABSTRACT

This paper investigates the influence of viscosity and viscoelasticity on the structure of the flow in a line vortex in view of understanding their effects on cavitation inception. Experiments were conducted in a vortex chamber where the fluid injection speed and the liquid properties can be easily controlled. Measurements of the velocities, pressures, and thus the cavitation number were conducted using a PIV system, pressure gauges, and Pitot tubes. Experiments were performed using water, different dilute concentrations of polymer (POLYOX WSR 301) solutions, and solutions with different concentrations of corn syrup for a large range of Reynolds numbers. The measurements and observations showed that cavitation inception at the vortex center was delayed when polymer and corn syrup solutions are used as compared to the experiments in water. However, contrary to reported observations with tip vortices, here the large scale vortex was found to rotate faster in the polymer and corn syrup solutions. This did not match with our observations of cavitation inception delay in the case of polymers and the conventional thinking about the relationship between pressures and velocities in a vortex line. This may be due to the observations that the velocity fluctuations and the turbulent kinetic energy in the viscous core region increased significantly in the polymer and corn syrup solutions and could question the validity of a pressure computation based on a single vortex.

INTRODUCTION

Tip vortex cavitation is typically observed as the first form of cavitation in propeller flows. The resulting risk for discretion of a naval vessel explains the desire to delay such cavitation inception. Laboratory tests have shown that a dilute solution of polymer everywhere in the liquid [1] can delay cavitation inception through both reduction of the vortex circulation and thickening and slowing down of the vortex viscous core. *Local* injection of polymer solutions in the tip region was also shown effective in delaying the tip vortex cavitation inception without affecting the lift. This was demonstrated on elliptic foils in [1]-[3], and on a full propeller in [4]. However, the mechanisms that resulted in the above described effects and inhibited the tip cavitation are not fully understood. Due to the complexity of a propeller flow, experimental measurements of the velocity in the core region of the rotating vortical structures are very challenging due to both the rotation motion and wandering of the vortex core. To study the problem in a controlled laboratory environment, we built a Plexiglas vortex chamber in order to generate and visualize a columnar vortex flow and conducted tests with water and various concentrations of viscous and viscoelastic additives. The vortex chamber had a circular cross section and the flow was injected tangentially through several uniformly distributed slots. The 'swirl' strength was controlled by the flow rate of the liquid in the loop. PIV measurements were conducted to characterize the flow in the chamber for several flow rates and with different solutions. This paper presents the results of these measurements and discusses the observed effects of viscosity and viscoelasticity on the vortex flow in the chamber.

EXPERIMENTAL SETUP AND APPROACH

The experiments were conducted in the chamber shown in Figure 1. The chamber consisted of two concentric cylinders. The fluid entered in the first cylinder, which served as a plenum, then was injected tangentially into the inner chamber through eight tangential slots. End plates with circular orifice openings were mounted on each end-side of the cylinder. When the flow rate exceeded a limit value, cavitation occurred at the center of the vortex and a tubular cavitation vortex line was observed between the two outlets as the flow rate was increased (see Figure 2). The chamber was set in a long tank filled with liquid and a close loop was set up with a recirculating pump. The liquid was supplied from the top of the chamber and it was then taken out from the middle and bottom of the tank such that it did not disturb the flow near the outlets of the swirl chamber. The schematic and dimensions of the setup are shown in Figure 3 and Table 1, and a picture of the actual setup and experimental equipment is shown in Figure 4.

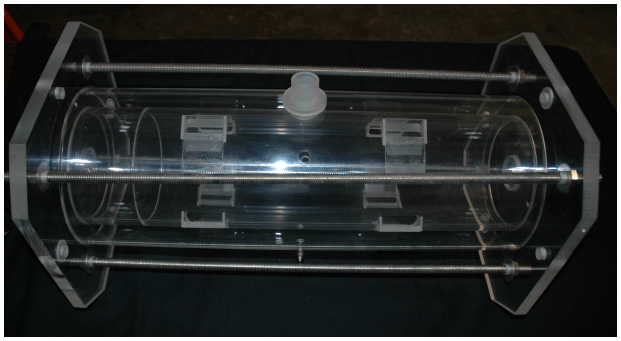

Figure 1: Picture of the vortex chamber

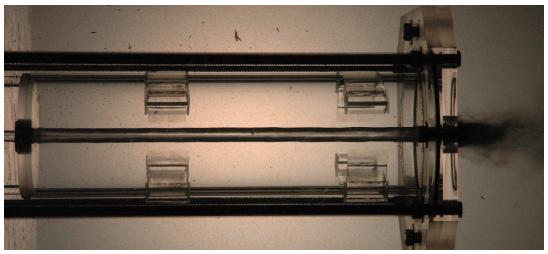

Figure 2: Picture of the vortex chamber at high flow rate with a large cavitation core in its center.

Inner cylinder ID	5.5 in
Outer cylinder OD	7.5 in
Inner and outer cylinder thickness	1/4 in
Slot width	1.85 in
Slot height	0.5 in
Outlet diameter	0.6 in
Chamber length	23.8 in
Wall - Chamber distance	12 in
Liquid level	12 in
Outlet-slot distance	5 in
Total number of slots	8
Angular positions of the slots	70^o, 160^o, 250^o, 340^o

Table 1: List of all the vortex chamber dimensions.

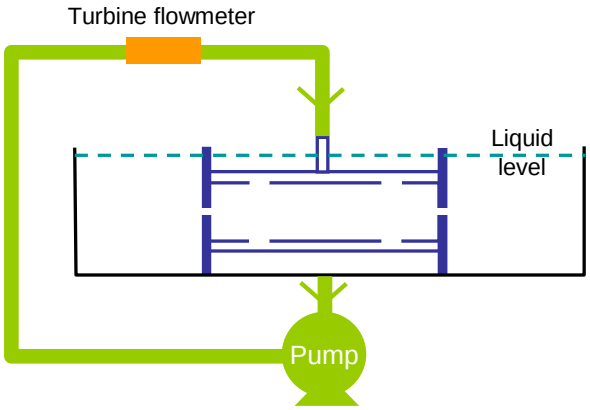

Figure 3: Schematic of the test loop.

An Oxford laser VisiVector E6 PIV system was used to perform the Particle Image Velocimetry (PIV) measurements. This system employed a HSI diode laser (15 mJ/pulse, 808 nm wavelength). A combination of spherical and cylindrical lenses was used to produce a laser sheet 30 mm wide and 2 mm thick

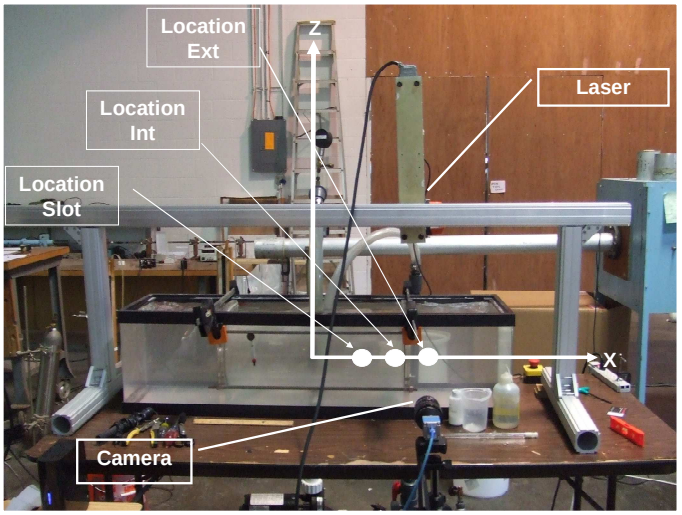

Figure 4: Picture of the setup and instrumentation

in the area of interest. The duration of a single laser pulse was 40-50 µs and the time between the pulses ranged between 400 µs at low flow rates to 10 µs at high flow rates.

A PCO Pixelfly-qe CCD camera with an AF Nikkor (Nikon) 35mm f2.0D lens with a teleconverter x2 set at about 2-2.5 ft from the mid-plane of the chamber was used to capture the PIV images. The camera had a resolution of 1,392x1,024 pixel (12-bit digital output) at 12 frames per second and a pixel width varying from 45 to 65 µm was achieved.

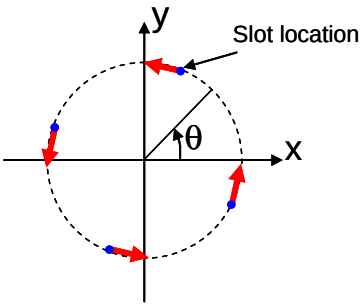

Figure 5: Definition of the angle θ and locations of the tangential slots (shown as red arrows) on the inner cylinder.

A commercial ViDPIV software was used for image acquisition and subsequent data post-processing. The calculation of instantaneous velocity vector maps was done by means of cross-correlation between two images: a first correlation, including a Whitaker peak fit and phase correlation [5]was performed on 48 x 48 (24 pixel shift) interrogation windows; then a local median filter was applied, and the resulting filtered vectors interpolated. An adaptive correlation function was applied on 24 x 24 pixel (12 pixel shift) interrogation windows; then a local median filter was applied.

As for the spatial resolution, the size of the evaluated area was approximately 30x50mm^2 with a spacing of 0.54-0.78 mm corresponding to 12 pixel units.

For each series of experiments, 200 image pairs were taken and averaged. Checks on the sufficiency of a 200 picture pair ensemble size were performed by increasing the ensemble

size to 300 picture pairs. However, no significant improvements in the mean values were observed.

Instantaneous profiles without time averaging and vector interpolations were also used to further understand the vortex dynamics.

PIV measurements were conducted in the mid-plane (Z=0) of the chamber with different fluids: pure water, homogeneous polymer solutions (from 50 to 1000ppm), and homogeneous corn-syrup solutions (9% and 12%, mass concentration). Along the length of the chamber, the vortex cross-section rotation velocity profile changed somewhat but not to a great extent. This is illustrated in Figure 6. In the rest of the paper we will only concentrate on the Z=0 profile.

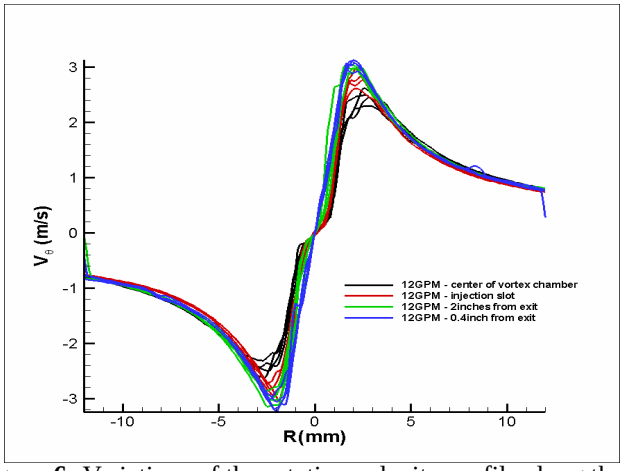

Figure 6: Variations of the rotation velocity profile along the vortex tube, here illustrated for a solution of 50ppm of Polyox at a flow rate or 12gpm.

For each experiment, a set of 200 instantaneous flow fields were averaged. For all the measurements, the vortex wandering was found to be small (less than 0.5 mm) and thus, no corrections were done for it. Typical averaged flow fields for low and high flow rates are shown respectively in Figure 8 and Figure 9. Using the streamlines, the center of the vortex was estimated with an error of at most 0.1mm. We can notice in the side edge regions of the figure the presence of four higher tangential velocity areas: these four high-speed areas correspond to the four slot injectors on the periphery of the inner cylinder. The angular positions of these areas correspond to the angular positions of the slots (Figure 5).

For each set of experiments, profiles were extracted along the lines $\theta = -\pi/4, 0, \pi/4$ and $\pi/2$ (see Figure 5 for θ definition). Each profile was fitted with a modified Rankine vortex function defined as:

$$\begin{aligned} V_\theta &= 0, && \text{if } r < a, \\ V_\theta &= (r-a)\omega, && \text{if } a \le r \le R_v, \\ V_\theta &= \frac{\Gamma}{2\pi r}, && \text{if } r > R_v, \end{aligned} \qquad (1)$$

where R_v, the viscous core radius, is the radial position where the max tangential velocity is observed, and the parameter a describes the size (radius) of the cavitation core when there is a cavity at the vortex line center (Figure 7).

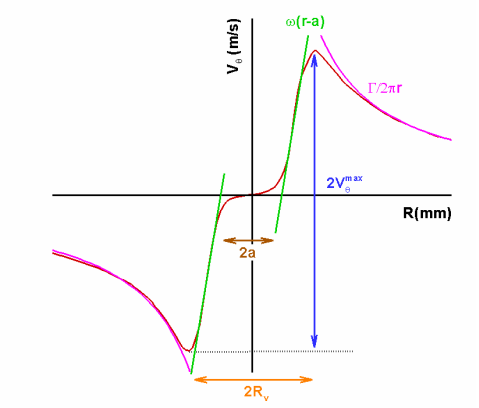

Figure 7: Definitions Γ, ω, R_v, a, and V_θ^{max}.

For brevity, only the results obtained with the profiles extracted at $\theta=\pi/4$ are shown here. The profiles extracted at the other locations are similar and showed similar trends.

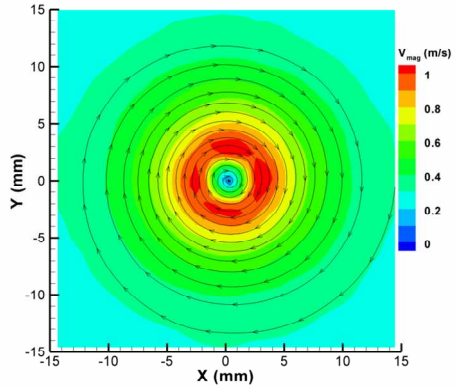

Figure 8: Contours of the mean velocity magnitude and its streamlines for water at 6gpm (V_{slot} = 0.089m/s).

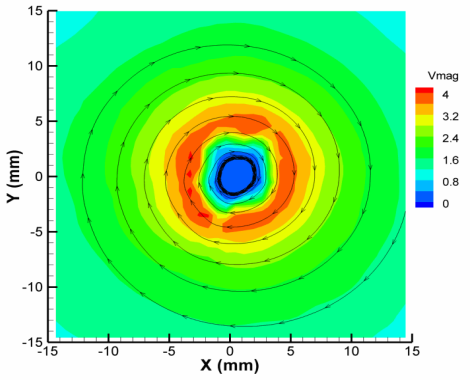

Figure 9: Contours of the mean velocity magnitude and its streamlines for water at 25.4gpm (V_{slot} = 0.356m/s)

RESULTS FOR WATER

Figure 10 shows the evolution of the tangential velocity profiles with increasing flow rate for the case of pure water at $\theta = \pi/4$. A cavitation core appears at about 12.3 GPM and rapidly fills the whole vortex centerline. As the flow rate increases, the cavitation core obtained from averaging the measurements in time grows in size.

Figure 11 shows two instantaneous flow fields measured at two different flow rates with water. For both flow rates, we can observe that the velocity near the center is not uniform in magnitude, underlying the non-axisymmetric behavior of the flow probably caused by the flow injection through slots.

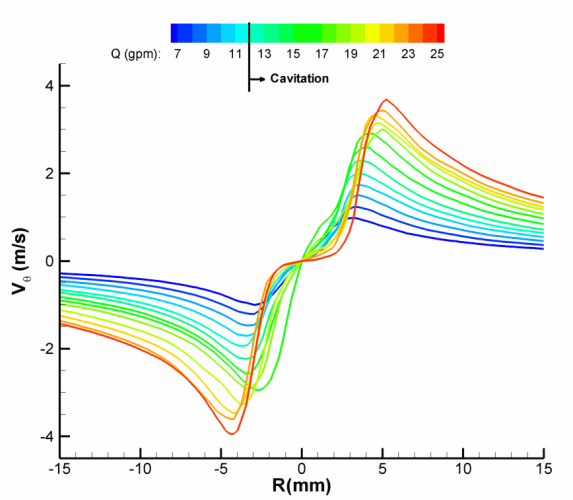

Figure 10: Profiles extracted at θ = π/4 with water for different water flow rate.

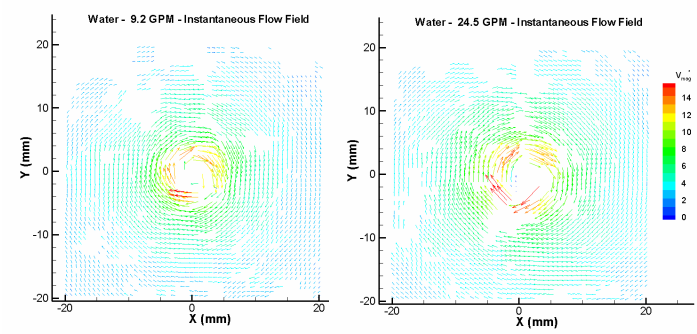

Figure 11: Instantaneous velocity vectors for two flow rates with water. The velocity magnitude has been dimensionalized by the velocity at the slot.

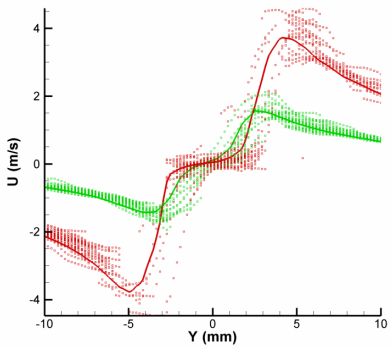

Figure 12: Mean velocity profiles extracted at θ=π/4 with water at 9.2 gpm (green line) and 24.5 gpm (red line). The symbols are 30 instantaneous velocity profiles at the corresponding flow rate.

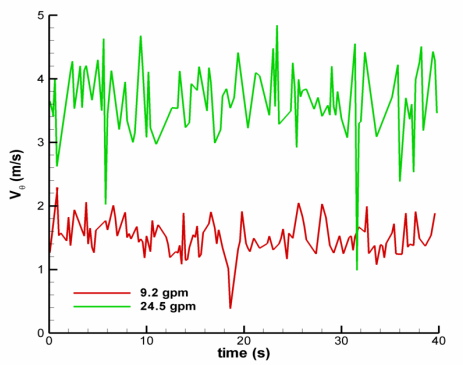

Figure 13: Time history of the tangential velocity for two flow rates with water at $R \sim R_v$

Figure 12 shows the mean velocity profiles extracted at θ=π/4 for the 9.2 gpm and 24.5 gpm water flow rates as well as 30 instantaneous profiles. This illustrates the strong time varying character of the viscous core as expressed using both the core radius and the maximum tangential velocity at this radius. Figure 13 shows the time history for two flow rates with water at a radial position near the viscous core. Large oscillations in the tangential velocity are observed.

Figure 14 shows the evolution of the viscous core radius, R_v, for increasing flow rate. The average liquid velocity at the slot was obtained by dividing the water flow rate by the total cross section area of all slots, 43.37cm^2. Before cavitation, which shows up in the red curve of Figure 14, when R_{cav} starts having a non-zero value, the viscous core radius shown in the green curve grew quasi-linearly with the flow rate. When cavitation occurred, the viscous core radius decreased noticeably at first, and then started growing quasi-linearly again as the flow rate continued to increase. Thus the appearance of the cavitation core caused an important effect on the velocity flow field in the vicinity of the vortex core edge. However, no effects were observed in the potential region $(R > R_v)$ or on the maximum tangential velocity, which continued growing monotonically with the flow rate.

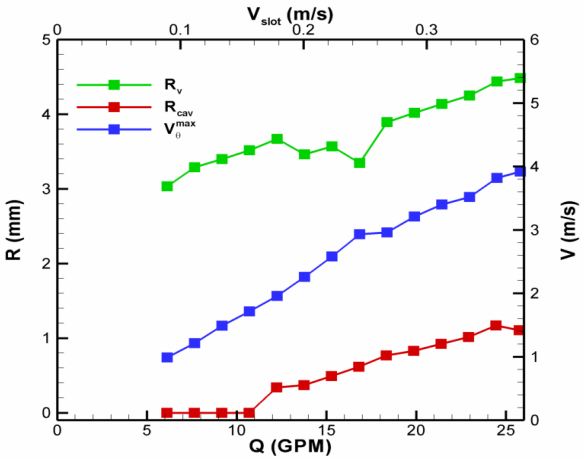

Figure 14: Evolution of the viscous core radius R_v, the cavitation core radius R_{cav}, and the maximum tangential velocity with the water flow rate.

RESULTS WITH POLYOX AND CORN SYRUP SOLUTIONS

The viscosities of the Polyox and the corn syrup solutions were measured with a falling ball viscometer. This was not meant to obtain the viscoelastic parameters for the Polyox (non-Newtonian) but was used only to compare the Newtonian viscosity measured with those of water and the corn syrup solutions. Comparison between the Polyox and the corn syrup at the same viscosity are meant to bring out any differences due to the viscoelasticity. The properties of the fluids and their temperature during the experiments are listed in Table 2.

Fluid	T (^{o}C)	μ (cP)	ρ (g/cm^3)	ν (cSt)
Water	16	1.11	1.0	1.11
Polyox 50 ppm	20	1.02	1.0	1.02
Polyox 250 ppm	20	1.32	1.0	1.32
Polyox 500 ppm	20	1.44	1.0	1.44
Polyox 750 ppm	20	1.62	1.0	1.62
Polyox 1000 ppm	20	1.84	1.0	1.84
Corn Syrup 9%	20	1.33	1.03	1.28
Corn Syrup 12%	20	1.47	1.04	1.40

Table 2: Properties of the different liquids used in this study.

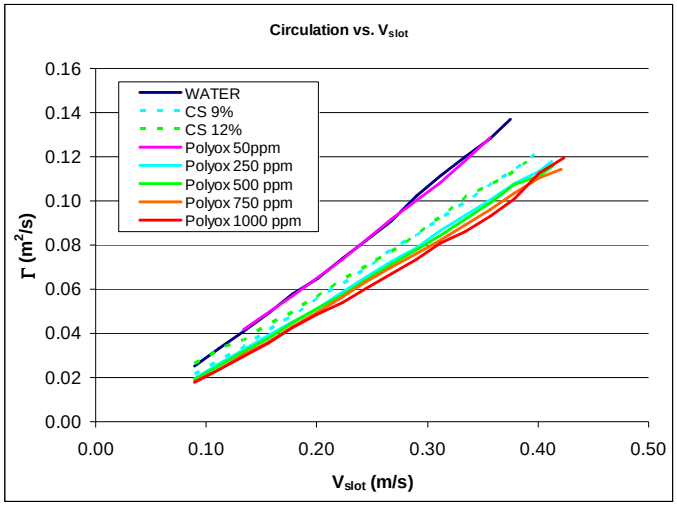

Figure 15: Circulation versus average injection velocity with the different liquids.

The following figures compare the differences in behavior of the liquids in the vortex chamber between water, and different concentrations of Polyox and corn syrup. Figure 15 shows that for a given pump flow rate (or slot average injection speed) there is a drop in circulation for the Polyox solutions when the concentration exceeds 250ppm. This implies that in order to decouple the effects of the additives on the loop from those on the line vortex, a correct comparison between different liquids should use the measured liquid circulation Γ in the potential flow region and not the injection velocity.

Figure 16 shows that for the same circulation, the maximum tangential velocity observed in the corn syrup and in the polymer solutions are higher than those in water. As the circulation is increased, the differences between the various liquids increase but the velocity profiles become also more and more turbulent (as shown later) and the errors on the maximum tangential velocity determination increase.

Figure 17 shows that for the same circulation, the viscous core radius became smaller as polymer and corn syrup solutions were added to the water. Also the corn syrup and polymer solution were found to rotate faster in the viscous core of the vortex line (Figure 18). Despite these observations, the cavitation inception was observed to be delayed in the cases of the viscous and viscoelastic solutions as shown in the plots of the cavitation bubble radius in Figure 17.

These results are contrary to expectations and to analysis as we expect the cavitation to occur when a maximum tangential (or rotation speed) is observed in the viscous core. This implies that the averaging procedure in space and time has obscured the physics of the flow in the vortex tube flow. Thus, it appears that the cavitation inception is related to small turbulent structures in the vortex core rather than to the mean flow field described above.

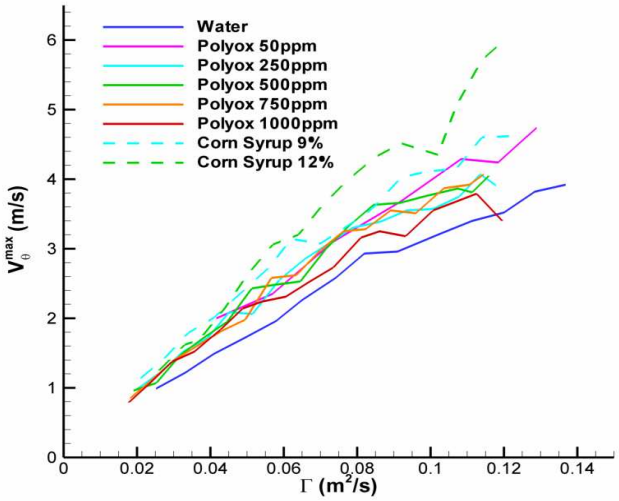

Figure 16: Maximum tangential velocity versus circulation for different liquids.

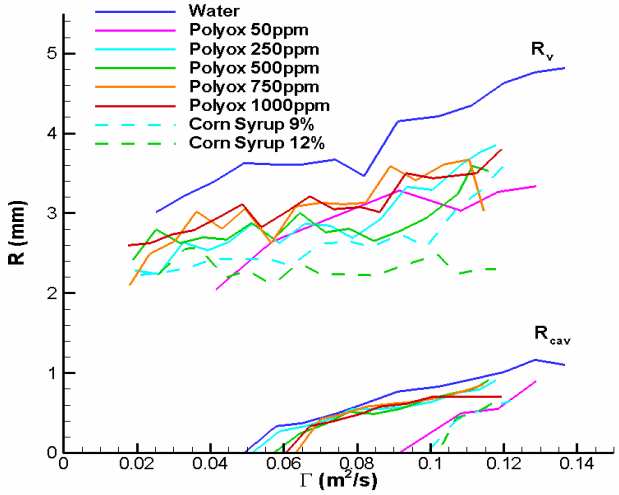

Figure 17: Viscous core and cavitation cylindrical bubble radius versus circulation for different liquids.

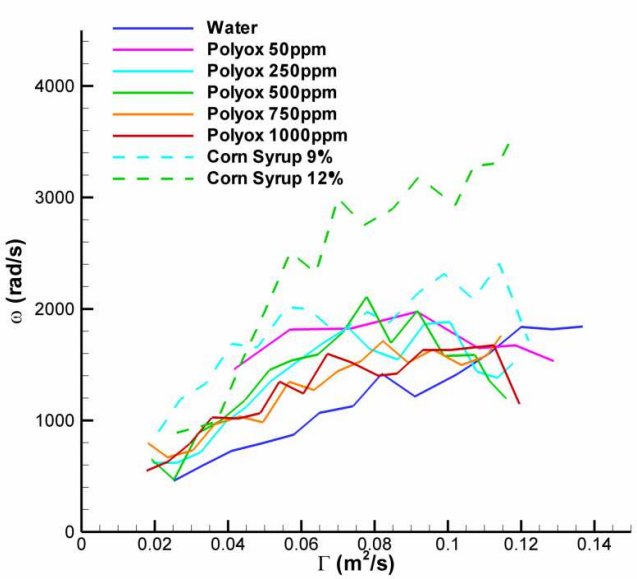

Figure 18: rotation speed in the viscous core for different liquids

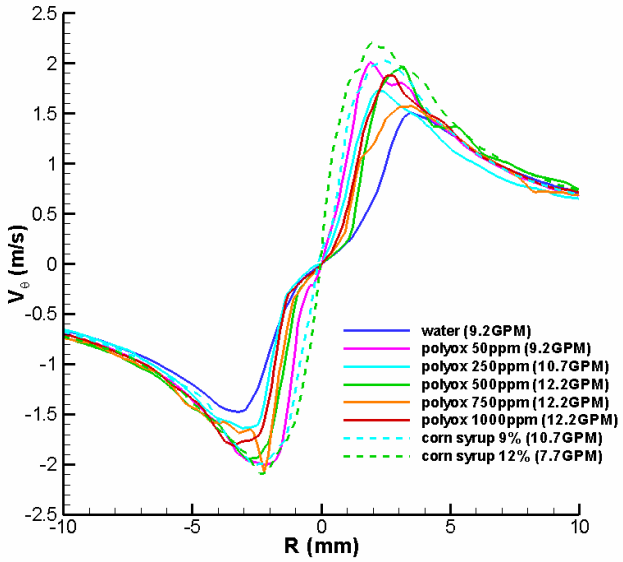

Figure 19: Mean velocity profiles for different liquids with approximately the same circulation ($\Gamma \sim 0.041 m^2/s$)

TURBULENT VELOCITY FLUCTUATIONS

To characterize the turbulence, a turbulent kinetic energy is deduced from the measurements using:

$$TKE = \frac{1}{2}(u_{rms}^2 + v_{rms}^2) \qquad (2)$$

where u_{rms} and v_{rms} are the root mean square of the velocity components in the (r,θ) PIV plan. The third velocity component in the vortex axial direction is neglected since the measurements are performed in the mid-plane where the axial velocity is nominally zero and negligible relative to the tangential velocity.

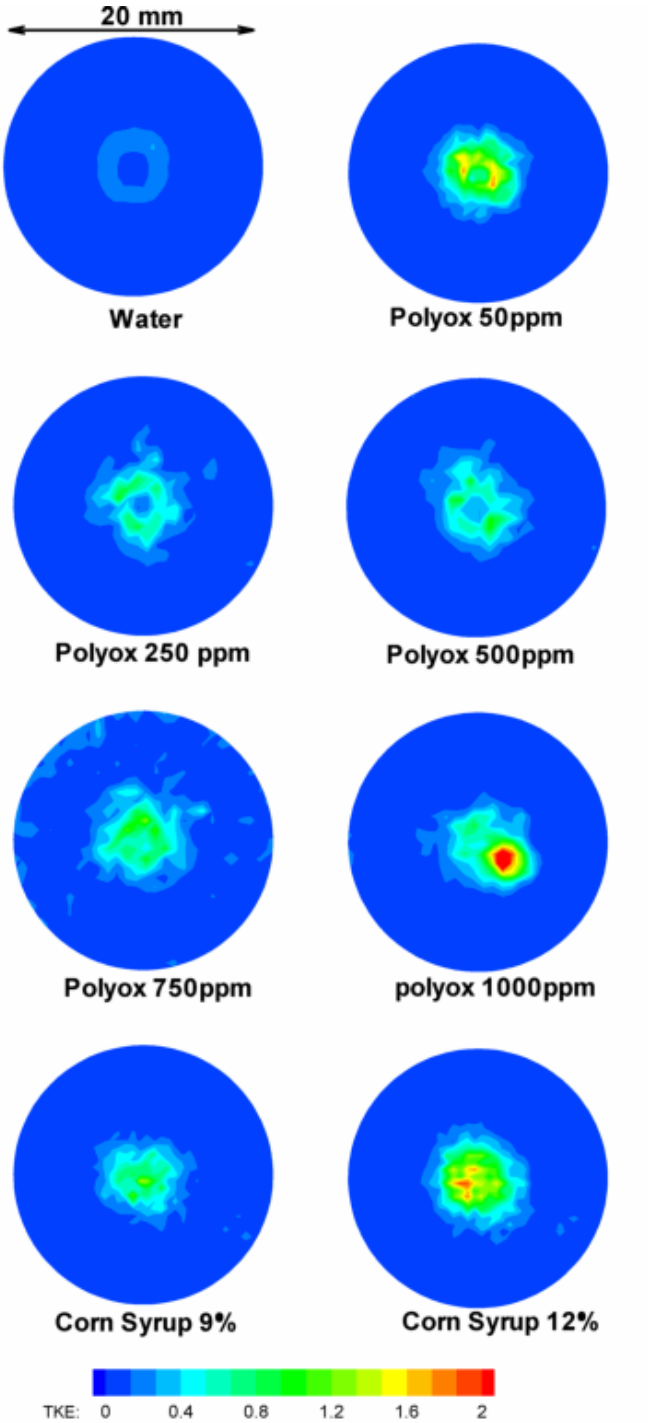

Figure 20: Turbulent kinetic energy in m^2/s^2 with different liquids for a flow rate of 9.2 GPM (no visible cavitation in the core of the vortex)

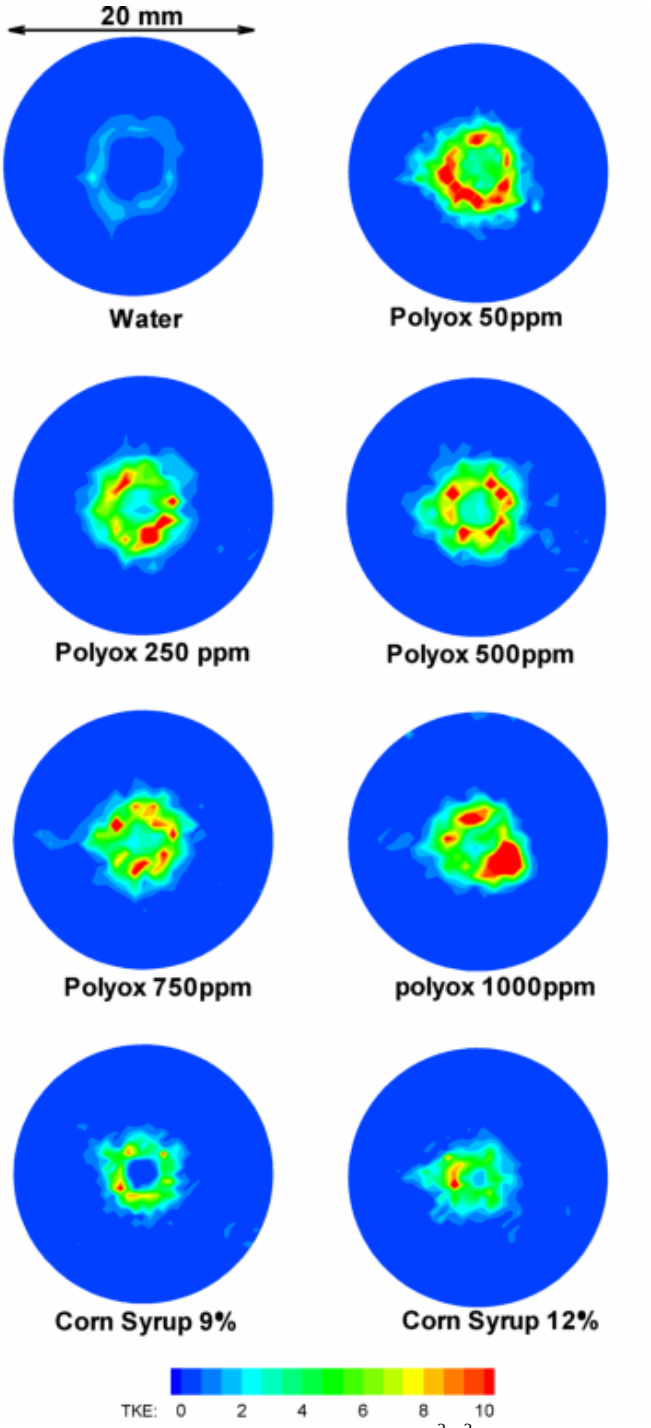

Figure 21: Turbulent kinetic energy in m^2/s^2 with different liquids for a flow rate of 24.5 GPM (cavitating vortex line core present for all the cases).

Figure 20 and Figure 21 show the turbulent kinetic energies for two flow rates: 9.2 GPM (V_{slot} = 0.134m/s) and 24.5GPM (V_{slot} = 0.356m/s). At 9.2 GPM, none of the liquids were cavitating, whereas at 24.5GPM, all the cases had a cavitation cylindrical bubble line at the center of the vortex line. The TKE is found to be much lower for both flow rates for pure water. With the other liquid solutions with additives high values of the TKE are found in the viscous core radius region (i.e. region of $v_{\theta,\max}$). There, the tangential velocities and the velocity fluctuations are the highest. These high values are also caused by observed fluctuations in times of the location of the viscous radius The increase of TKE observed for the corn syrup can be explained by the highest rotation speed observed in the corn syrup solutions. This is counter-intuitive as we would expect the flow to be more stable at higher viscosity since the Reynolds number is lower.

As shown in Figure 22, the TKE values observed at 50 and 1,000ppm are very similar. Overall, it seems that the viscoelasticity effects saturate for solution concentrations higher than 250ppm. The TKE is found to be 10 times smaller in water than in the other solutions (see Figure 22).

The importance of the effect of turbulence on cavitation inception has been already reported in various contributions, including for marine propellers (e.g. [6]), which found that the cavitation inception number increased with increasing turbulence intensity in the free stream. They found that altering the free stream turbulence had a similar effect on the cavitation inception as using leading-edge roughness technique.

Defining the turbulence intensity by:

$$TI(\%) = 100\frac{\sqrt{u_{rms}^2 + v_{rms}^2}}{\sqrt{U_{mean}^2 + V_{mean}^2}}, \qquad (3)$$

we can investigate the overall turbulence outside of the vortex region where the velocity is close to zero. Figure 23 and Figure 24 show the turbulence intensity for selected low and high flow rates. For clarity, the values in the center of the vortex are blanked in Figure 23 and Figure 24 to avoid division by very small numbers. The turbulence in water is found to be more uniform than for the other solutions.

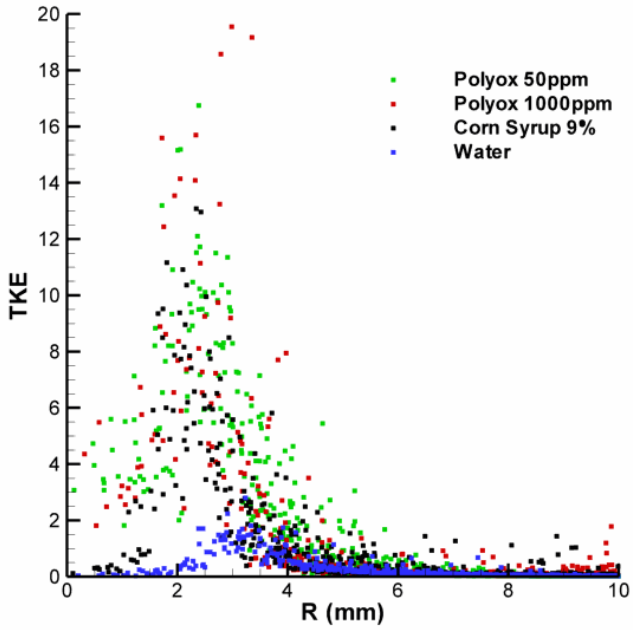

Figure 22: Turbulent kinetic energy for a flow rate of 25.4 GPM for water and various viscous solutions.

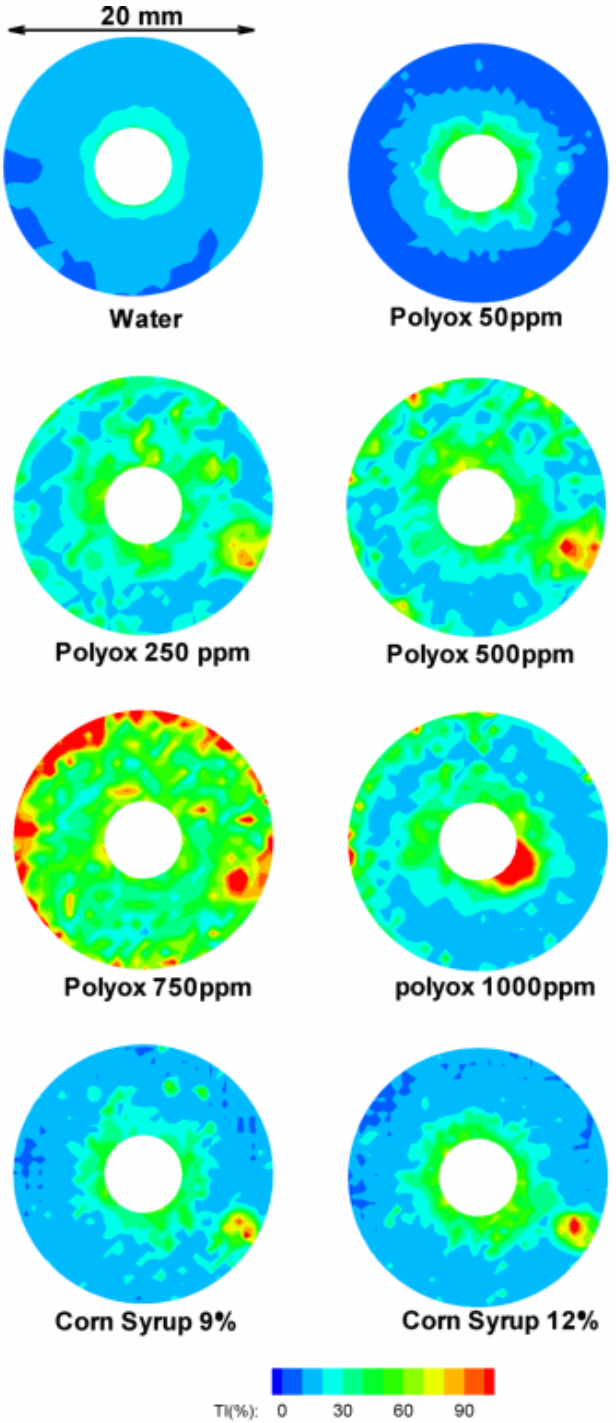

Figure 23: Turbulence intensity (%) with different liquids for a flow rate of 9.2 GPM (no cavitation core in the chamber).

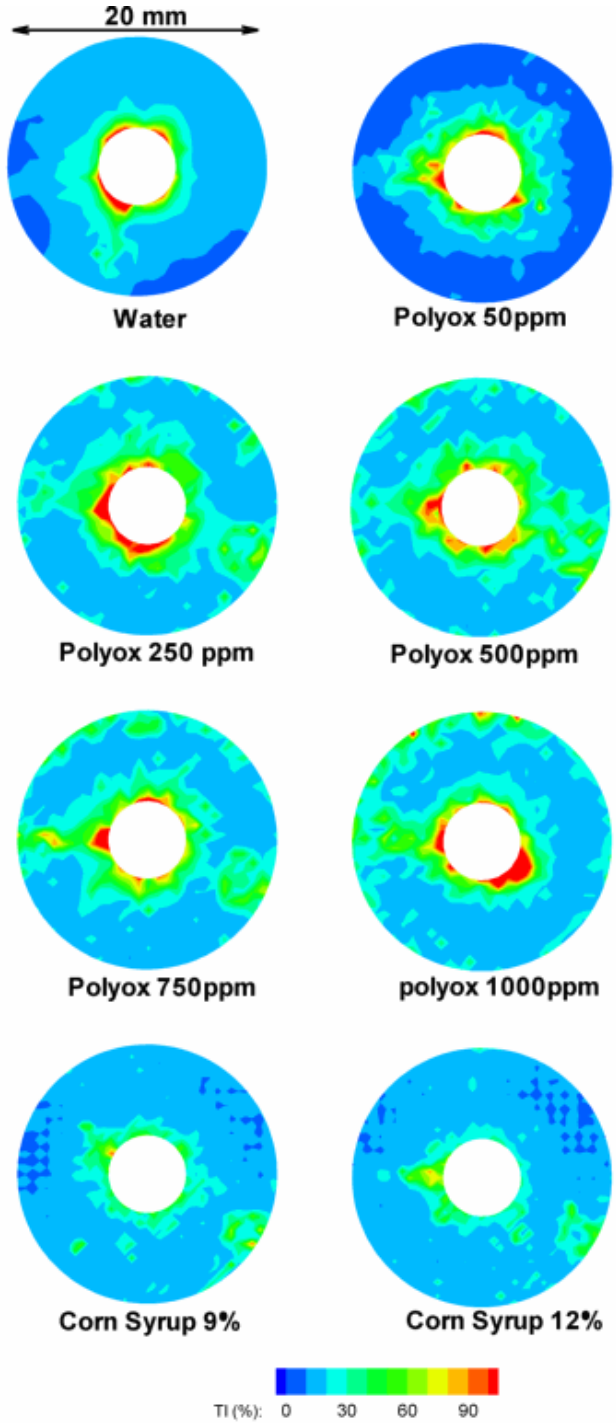

Figure 24: Turbulence intensity (%) with different liquids for a flow rate of 24.5 GPM (cavitation core present for all the cases).

CONCLUSIONS

A vortex chamber with tangential injection was used to generate a central line vortex and observe its structure in water and various solutions of polymer and corn syrup. While the vortex chamber appeared to be of a large enough size and good quality to allow easy observation of cavitation inception and bubble dynamics, it turned out to still present difficulties for fine detailed studies of the vortex structure.

Due to strong velocity fluctuations, vortex core size oscillations, and potential presence of more than one vortex structure, averaging the data in time appears to result in unexpected trends, which cannot yet be confirmed with full confidence, especially that these fluctuations (as well as measurements errors) increase significantly in the presence of viscous solutions. This is clearly seen in the evaluations of the turbulent kinetic energies and the turbulence levels. The delay in the cavitation inception in the vortex chamber with polymer

and corn syrup appear to be a consequence of this increase in turbulent kinetic energy, rather than a decrease in the rotational speed or a growth of the viscous core. However, these results are tentative and need to be revisited with an approach, which does not consider averaging the raw data, but rather conducting analysis on the instantaneous data. This is tedious, unless automated, and will be one of our near future tasks.

ACKNOWLEDGMENTS

This work was conducted at DYNAFLOW, INC. (*www.dynaflow-inc.com*) and was supported by the Office of Naval Research under contract No. N00014-08-C-0448 monitored by Dr. Ki-Han Kim. We gratefully appreciate this support. We would like to thank Stephane Causse, summer student at DYNAFLOW, for helping with the conduct of experiments and analysis.

REFERENCES

[1] Fruman, D. and Aflalo, S., "Tip Vortex Cavitation Inhibition by Drag Reducing Polymer Solution", J. Fluid Engr. Vol. 111, pp.211-216, 1989.

[2] Fruman, D.H., Pichon, T. and Cerrutti, P., "Effect of a Drag-reducing Polymer Solution Ejection on Tip Vortex Cavitation", J. Mar. Sci. Tech., 1, pp.13-23, 1995.

[3] Latorre, R., Muller, A., Billard, J.Y. and Houlier, A., "Investigation of the Role of Polymer on the Delay of Tip Vortex Cavitation", J. Fluid Engr., 126, pp.724-729, 2004.Wernet, M., 2005, "Symmetric phase only filtering: a new paradigm for DPIV data processing", Meas. Sci. Technol., 16, 601-618.

[4] Chahine, G.L., Frederick, G.F. and Bateman, R.D., "Propeller Tip Vortex Cavitation Suppression Using Selective Polymer Injection", J. Fluid Egnr., 115, pp.497-503, 1993.

[5] Wernet, M., 2005, "Symmetric phase only filtering: a new paradigm for DPIV data processing", Meas. Sci. Technol., 16, 601-618.

[6] Korkut, E., and Atlar, M., "On the Importance of the Effect of Turbulence in Cavitation Inception Tests of Marine Propellers", Proc. R. Soc. Lond. A, 2002, 458, pp 29-48.